ISSN 0024-4902, Lithology and Mineral Resources, 2006, Vol. 41, No. 1, pp. 1–14. © Pleiades Publishing, Inc., 2006.
Original Russian Text © A.V. Dubinin, T.Yu. Uspenskaya, 2006, published in Litologiya i Poleznye Iskopaemye, 2006, No. 1, pp. 3–18.

Geochemistry and Specific Features of Manganese Ore Formation in Sediments of Oceanic Bioproductive Zones

A. V. Dubinin and T. Yu. Uspenskaya

Shirshov Institute of Oceanology, Russian Academy of Sciences,
Nakhimovskii pr. 36, Moscow, 117997 Russia
e-mail: dubinin@sio.rssi.ru

Received May 23, 2005

Abstract—Processes of authigenic manganese ore formation in sediments of the northern equatorial Pacific are considered on the basis of study of the surface layer (<2 mm) of ferromanganese nodule and four micronodule size fractions from the associated surface sediment (0–7 cm). Inhomogeneity of the nodule composition is shown. The Mn/Fe ratio is maximal in samples taken from the lateral sectors of nodule at the water–sediment interface. Compositional differences of nodules are related to the preferential accumulation of microelements in iron oxyhydroxides (P, Sr, Pb, U, Bi, Th, Y, and REE), manganese hydroxides (Co, Ni, Cu, Zn, Cd, Mo, Tl, W), and lithogenous component trapped during nodule growth (Ga, Rb, Ba, and Cs). The Ce accumulation in the REE composition is maximal in the upper and lower parts of the nodule characterized by the minimal Mn/Fe values. The compositional comparison of manganese micronodules and surface layers of the nodule demonstrated that the micronodule material was subjected to a more intense reworking during the diagenesis of sediments. The micronodules are characterized by higher Mn/Fe and P/Fe ratios but lower Ni/Cu and Co/Ni ratios. The micronodules and nodules do not differ in terms of contents of Ce and Th that are least mobile elements during the diagenesis of elements. Differences in the chemical composition of micronodules and nodules are related not only to the additional input of Mn in the process of diagenesis, but also to the transformation of iron oxyhydroxides after the removal of Mn from the close association with Fe formed in the suspended matter at the stage of sedimentation.

DOI: 10.1134/S0024490206010019

Ferromanganese formations in sediments are derived from hydrogenous suspended matter formed at the upper layer of oceanic water column (Dubinin, 2004; Sholkovitz *et al.*, 1994). The suspended matter usually contains fine intergrowths of iron and manganese oxyhydroxides that are good sorbents. Therefore, they readily adsorb microelements, particularly Co and Ce. Like Mn, these elements are accumulated due to the successive processes of sorption and oxidation (Moffett, 1990; Moffett and Ho, 1996). With increasing depth with sedimentation, Mn, Co, and Ce are reduced by organic matter that is always present in the suspended matter (Dubinin, 2004). Transformation of the suspended matter persists under postsedimentary conditions on the seafloor. Consequently, the iron and manganese oxyhydroxides are transformed into independent authigenic mineral aggregates (ferromanganese nodules and manganese micronodules). Their composition depends on chemical reactions in both sediments and nodule surface. This is indicated by the compositional inhomogeneity of the upper and lower parts of nodules. The lower part is allegedly formed under a strong influence of the diagenetic scavenging of material from the sediment. Micronodules grow on the upper sedimentary layer under the influence of the same diagenetic processes that took place in the lower part, using the labile portion of sediment as material for their growth. Since the lower parts of both nodules and micronodules are products of the diagenesis of a compositionally analogous material, their compositions should be sufficiently similar. However, it is well known that the composition of micronodules varies significantly depending on their size (Dubinin, 2004).

Comparison of nodules and micronodules located in sediments at a certain station makes it possible to elucidate processes of the formation of ferromanganese formations during the diagenesis at similar fluxes of the suspended matter. Since the nodules and micronodules differ in size, one cannot consider them coeval formations. If we assume that they grow at an approximately equal rate, only the surface layer of a nodule with thickness similar to that of micronodule radius can be formed at a certain time interval.

The majority of methods for the determination of nodule growth rate show that the growth rate is only *n* mm/Ma, whereas sedimentation rate in the same area is at least three orders of magnitude higher (Baturin, 1986; Baturin and Savenko, 1989; Volkov, 1979). Hence, one can suppose that ancient formations (nodules) are located on younger associated sediments. Recent datings of nodules in the northern equatorial zone based on cosmogenic isotopes of noble gases show that nodule growth and sedimentation rates have

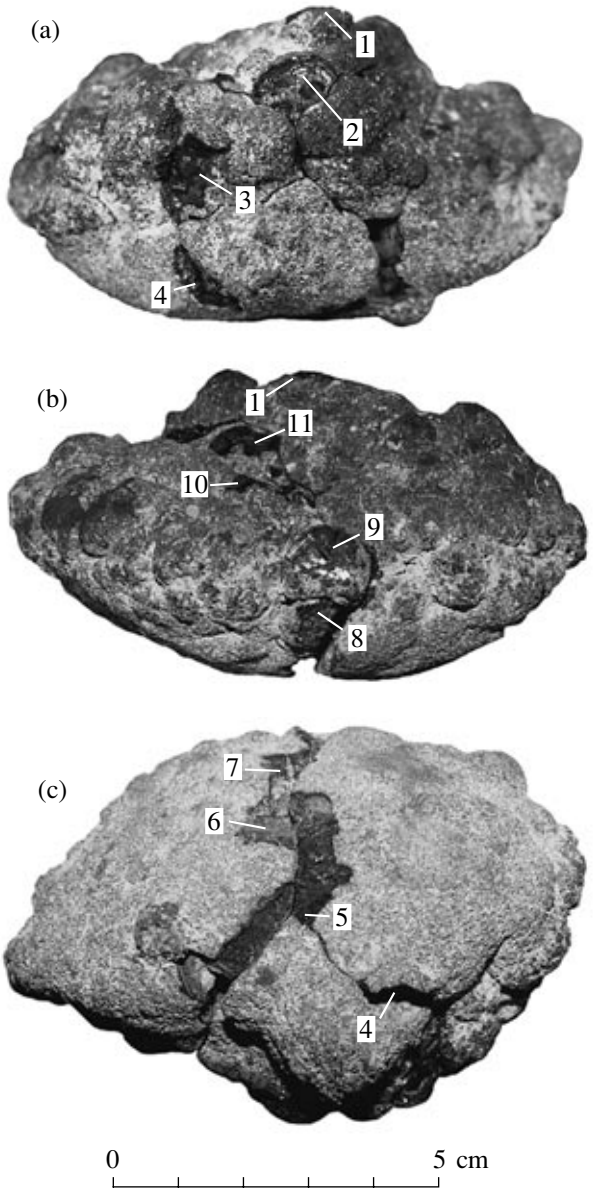

Fig. 1. Sampling points in the surface layer (<2 mm) of a ferromanganese nodule from Station 3911/76: (a) lateral front view, (b) lateral back view, (c) view of the lower part of the nodule surface. Numbers near the sampling point are as in Table 1.

the similar order of approximately 1 mm/ka (Anufriev *et al.*, 1996). If we accept that both nodules and associated sediments are coeval, comparison of the sediment-facing lower parts of nodules and micronodules in this sediment is quite valid. This type of analysis can provide new insights into the formation mechanism of authigenic ferromanganese formations in pelagic sediments.

The aim of this communication is to study variations in the chemical and mineral compositions of the surface layer (<2 mm) of a ferromanganese nodule depending on its position in the sediment and to analyze relationship of chemical compositions of nodules and micronodules of different fractions in sediments of the northern equatorial Pacific.

MATERIALS AND METHODS

Material for the study was taken with an *Ocean-50* box corer during cruise 41 of the R/V *Dmitry Mendeleev* in 1988 at Station 3911/76 in the Northeast Basin of the Pacific (Clarion–Clipperton ore province) within the equatorial belt of biogenic silica accumulation (bioproductive zone) (Sval'nov, 1991).

At Station 3911/76 (13°26.92′ N, 132°54.29′ W; depth 4900 m), the sediments are composed of light brown clayey–radiolarian oozes enriched in diatoms at the surface interval (0–2 cm). The sediment surface includes sedimentary-diagenetic *oblate* ferromanganese nodules with an asymmetric section owing to the development of thinner layers in the upper part (Uspenskaya and Skornyakova, 1991). Sediments from Station 3911/76 (intervals 0–2 and 2–7 cm) and bulk composition of ferromanganese nodules have been studied in (Dubinin and Sval'nov, 2003). The present communication is devoted to the study of a large nodule ($9 \times 6.5 \times 5$ cm) recovered from sediments at Station 3911/76.

The studied *oblate* nodule is characterized by prominent morphological differences between surfaces oriented toward the bottom water and sediment. The samples were taken from the surface layer (<2 mm) along the meridional section of the ferromanganese nodule (Fig. 1). Samples 1–3 and 9–11 were taken from the upper (bottom water-facing) part, while samples 4–8 were taken from the lower (sediment-facing) part. Sample 6 was taken from an approximately 2-mm-thick swell on the lower part.

Air-dry samples of the ferromanganese nodule were ground before the chemical analysis. The nodule sample (approximately 30 mg) was treated in a mixture of concentrated HF, HNO_3, and $HClO_4$ in Teflon vessels with lids at 93°C for 7 h. Mn(IV) oxide precipitated in the course of ferromanganese nodule decomposition was reduced in 1 ml of 6M HCl and transferred to carbon crucible. After evaporation at 180°C, a mixture of concentrated HNO_3 and $HClO_4$ was repeatedly added to the crucible. Then, the samples were transferred to 5 vol % HNO_3 solution and used for the ICP-MS analysis of REE, Li, Be, Ga, Rb, Sr, Cd, Cs, Ba, Mo, W, Tl, Pb, Y, U, and Th with a PlasmaQuad PQ2STE inductively coupled plasma mass spectrometer, Fisions Instruments Co. (Dubinin, 1993; Strekopytov and Dubinin, 1997). Concentrations of Fe, Mn, Co, Ni, Cu, Zn, and Al were determined in the same samples with a SpectrAA220 atomic absorption analyzer, Varian Co. The accuracy of measurements was 3–5 rel %. The P content was determined by the spectrophotometric method based on the color intensity of P–Mo–Sb complex with a reproducibility of 3 rel %. Accuracy of the applied methods was checked by the analysis of standards

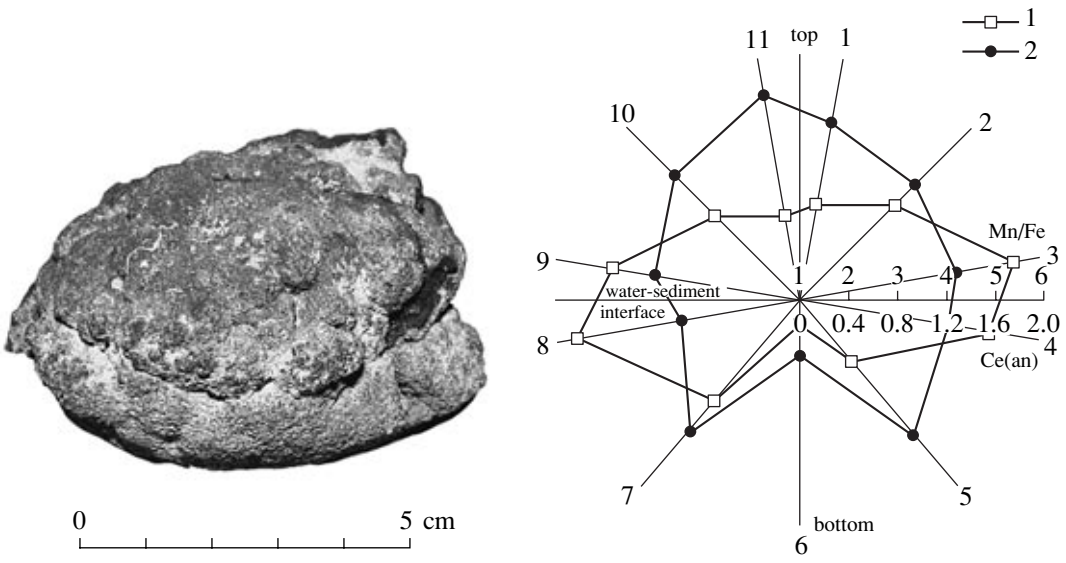

Fig. 2. Lateral view of a nodule from Station 3911/76 and distribution of (1) Mn/Fe and (2) Ce(an) values in the surface layer (<2 mm) in polar coordinates (the ratio is shown along the axis directed from the nodule center to the sampling point on the nodule surface).

SDO-9 (red deep-water clay), SDO-5 (ferromanganese nodule), and SDO-2 (volcanogenic–terrigenous silt).

The mineral composition of samples was analyzed by the SAED and energy-dispersive modifications of the TEM method at the Institute of Geology of Ore Deposits, Petrography, Mineralogy, and Geochemistry of the Russian Academy of Sciences (A.V. Sivtsov, analyst).

RESULTS

Chemical and mineral compositions are given in Tables 1 and 2, respectively. Variations in the REE content are shown as Ce anomaly, $Ce(an) = 2 \times Ce/Ce^{NASC}/(La/La^{NASC} + Nd/Nd^{NASC})$; the LREE/HREE ratio, as $(L/H)^{NASC} = (La/La^{NASC} + 2 \times Pr/Pr^{NASC} + Nd/Nd^{NASC})/(Er/Er^{NASC} + Tm/Tm^{NASC} + Yb/Yb^{NASC} + Lu/Lu^{NASC}$; and the Eu anomaly, as $Eu(an) = 2 \times Eu/Eu^{NASC}/(Sm/Sm^{NASC} + Gd/Gd^{NASC})$, where NASC is the North American Shale Composite (Gromet *et al.*, 1984).

At first glance, the major elements (Fe, Mn, and Al) vary insignificantly in different samples of the ferromanganese nodule, irrespective of the position of sampling point on the nodule surface (i.e., above or beneath the water–seafloor interface) (Fig. 1). The Fe content varies from 4.28 to 8.08%; the Mn content (except for Sample 6), from 20.1 to 26.2%. Minimal contents are recorded in samples taken from both upper and lower parts of the nodule. Sample 6 (Al 5.83%, Mn 6.44%) is probably dominated by the aluminosilicate matter of the underlying sediment entrapped in the course of nodule growth. These data are also confirmed by the mineral composition of this sample (Table 2). Other samples taken from the lower part of the sediment-facing nodule are enriched in Al (2.06–2.58%) relative to the bottom water-facing parts of the nodule (1.51–1.93%).

The Mn/Fe ratio depends on the position of the sampling point relative to the water–sediment interface. Minimal Mn/Fe values are recorded in the upper and lower parts of the nodule. They gradually increase toward the water–sediment interface (Fig. 2) and attain the maximal values in sampling points located above and beneath the interface. The minimal Mn/Fe value has been detected in Sample 6 because of the contamination of ferromanganese oxyhydroxides with the clayey material.

The behavior of microelements is governed by their links with macrocomponents in the ferromanganese nodule. With respect to the number of elements in the material and nodule matrix, we can identify three groups of microelements (Fe, Mn, and Al). Based on correlation analysis, the iron group includes P, Sr, Pb, U, Bi, Th, Y, and REE (Fig. 3). The manganese group includes Co, Ni, Cu, Zn, Li, Sr, Cd, Mo, Tl, and W (Fig. 4). The aluminum group (lithogenic aluminosilicate source) includes Ga, Rb, Ba, and Cs (Fig. 5). Beryllium does not fall into any group indicated above. Increase in the Mn/Fe value during diagenesis promotes increase in contents of microelements of the manganese group and decrease in contents of elements of the iron group.

REE distributions in the nodule are shown in Fig. 6. They are enriched in MREE relative to NASC. Except for samples 6 and 8, the REE spectrum shows a significant positive Ce anomaly. Variations in Ce anomaly are shown in Fig. 2. If Sample 6 appreciably contaminated with the clayey material is omitted from the consideration, one can see that the maximal Ce anomaly is recorded in both upper and lower parts of the nodule,

Table 1. Contents of elements and some relationships between them in the surface layer (<2 mm) of a ferromanganese nodule at Station 3911/76

Element	Sample no.										
	1	2	3	4	5	6	7	8	9	10	11
Fe	7.69	6.52	4.78	5.31	7.61	4.28	6.21	4.67	5.18	6.56	8.08
Mn	22.8	24.5	26.0	26.2	20.1	6.44	23.0	26.1	25.2	22.6	22.3
Al	1.52	1.70	1.93	2.06	2.58	5.83	2.37	2.31	1.92	1.92	1.51
Co	0.270	0.257	0.283	0.202	0.246	0.067	0.229	0.263	0.329	0.259	0.339
Ni	1.019	1.131	1.409	1.401	1.001	0.234	1.232	1.519	1.300	1.074	1.000
Cu	0.709	0.823	0.940	1.142	0.746	0.279	0.990	1.238	0.926	0.753	0.508
Zn	0.108	0.114	0.125	0.127	0.081	0.031	0.096	0.112	0.119	0.099	0.117
P	0.144	0.114	0.103	0.094	0.122	0.087	0.116	0.092	0.110	0.130	0.153
La	131	107	78.5	97.0	137	83.3	107	83.1	85.3	115	132
Ce	483	361	261	301	488	91.6	370	204	259	438	563
Pr	41.6	35.0	25.4	30.9	42.7	25.4	34.7	27.0	27.2	39.6	42.6
Nd	161	134	101	121	166	98	130	104	107	155	163
Sm	40.5	33.7	25.9	31.1	41.3	21.2	31.5	25.5	27.2	40.6	40.6
Eu	10.0	8.21	6.23	7.53	9.81	4.60	7.60	6.24	6.57	9.68	9.61
Gd	38.6	32.2	23.9	28.3	37.6	19.3	30.7	25.2	26.4	37.8	36.6
Tb	5.86	4.71	3.59	4.29	5.65	2.56	4.40	3.69	3.95	5.62	5.54
Dy	32.4	26.5	21.0	25.3	32.0	14.4	26.0	21.2	22.2	33.2	30.9
Ho	5.88	4.98	3.85	4.48	5.64	2.61	4.77	3.84	4.12	6.10	5.43
Er	16.0	13.6	10.7	11.9	14.9	6.70	12.9	10.4	11.1	16.2	14.3
Tm	2.20	1.92	1.48	1.73	2.11	0.89	1.75	1.46	1.54	2.27	1.96
Yb	14.7	12.2	9.64	11.0	13.5	5.50	12.1	9.39	10.0	14.8	12.6
Lu	2.13	1.84	1.44	1.75	2.10	0.81	1.81	1.38	1.56	2.26	1.88
Li	132	131	125	152	96	40	119	151	137	136	124
Be	1.5	1.0	0.9	1.3	2.1	1.5	1.6	1.3	1.2	1.6	1.6
Ga	62	61	58	95	83	212	89	88	69	73	57
Rb	16.8	22.2	22.3	22.0	21.3	48.1	21.2	22.2	19.8	17.1	14.4
Sr	621	549	483	477	519	207	468	415	470	544	599
Y	90	82	64	68	81	58	73	62	67	88	80
Mo	446	445	418	427	357	95	407	457	378	367	272
Cd	17.7	17.4	15.5	16.9	7.8	2.4	13.1	15.8	13.8	12.2	11.0
Cs	1.5	1.7	2.1	2.0	1.9	2.7	1.7	2.0	1.8	1.5	1.2
Ba	1209	1189	1065	1861	1763	4772	1782	1675	1464	1560	1197
W	45	36	38	58	50	17	53	52	41	36	39
Tl	135	192	165	166	76	20	145	199	128	162	83
Pb	566	506	439	356	560	73	434	407	442	578	687
Bi	7.8	6.0	5.8	6.1	10.8	0.6	7.9	4.4	5.5	9.4	9.7
Th	35.8	26.5	22.9	25.0	38.3	5.4	26.2	15.6	25.1	42.0	45.6
U	6.5	4.8	4.0	4.2	4.9	0.8	4.5	4.0	4.8	5.9	5.8
Mn/Fe	3.0	3.8	5.4	4.9	2.6	1.5	3.7	5.6	4.9	3.4	2.8
P/Fe	0.019	0.017	0.021	0.018	0.016	0.020	0.019	0.020	0.021	0.020	0.019
Co/Ni	0.27	0.23	0.20	0.14	0.25	0.29	0.19	0.17	0.25	0.24	0.34
Ni/Cu	1.44	1.37	1.50	1.23	1.34	0.84	1.24	1.23	1.40	1.43	1.97
Ce(an)	1.47	1.34	1.30	1.23	1.44	0.45	1.40	0.97	1.20	1.44	1.70
L/H	1.07	1.04	0.98	1.03	1.16	1.66	1.07	1.06	1.00	0.98	1.23
Eu(an)	1.11	1.09	1.10	1.11	1.09	1.00	1.07	1.08	1.08	1.08	1.09

Note: Contents of Fe, Mn, Al, Co, Ni, Cu, Zn, and P are given in %; others in ppm.

while the minimal Ce anomaly is observed beneath and above the water–sediment interface where the Mn/Fe value is maximal. The contamination with associated sediments results in correlation between Al and L/H value that characterizes the relative behavior of LREE and HREE, because the lithogenic component in the nodule is more enriched in LREE relative to HREE (Dubinin, 1998a; Dubinin and Strekopytov, 2001).

DISCUSSION

Nature of the Spatial Inhomogeneity of Ferromanganese Nodule

It is well known that the upper and lower parts of ferromanganese nodules are differently enriched in Fe and Mn (Dubinin and Strekopytov, 1994; Dymond *et al.*, 1984; Elderfield *et al.*, 1981; Skornyakova, 1986). During the oxidation of organic matter in the course of diagenesis, Mn is reduced prior to Fe:

$$\equiv\text{Fe-O-Mn-(OH)}_3 + \text{C(H}_2\text{O)}$$

$$\Rightarrow \equiv\text{Fe–OH} + \text{Mn}^{2+}_{\text{sol}} + \text{CO}_2 + 2\text{H}_2\text{O},$$

where ≡Fe–OH designates the surface composition of iron oxyhydroxides. Depending on the redox environment in sediments, the reduced Mn in interstitial waters can be transferred to either the lower part of the ferromanganese nodule or the bottom water, where this element is again oxidized and transferred to the upper part immediately overlying the water–seafloor interface. Such compositional differences are typical of sedimentary–diagenetic nodules in the Peru and Guatemala basins and the Clarion–Clipperton Fracture Zone (Dubinin and Strekopytov, 1994; Dymond *et al.*, 1984; Elderfield *et al.*, 1981; Skornyakova, 1986). The delivery of Mn, which was reduced during the early diagenesis of sediments, from the interstitial and bottom waters to the nodule surface leads to increase in Mn/Fe values and the consequent increase in the nodule growth rate

Table 2. Mineral composition of surface samples (<2 mm) of ferromanganese nodule at Station 3911/76

Sample no.	Mn/Fe	Mineral composition							
		Vernadite	Fe-vernadite	Asbolane-buserite	Birnessite	Fe-X	Amorphous SiO_2	Nontronite	Aluminosilicates
1	3.0	+	+	**s**		**s**	+	+	
2	3.8	+			**s**			+	
3	5.4	+			**s**			+	
4	4.9	+	+		+				+
5	2.6	+	+						+
6	1.5		+						+
7	3.7	+	+	**s**	**s**				+
8	5.6	+	+	**s**	**s**				+
9	4.9	+	+	**s**					
10	3.4	+	+			**s**			
11	2.8	**s**	+			+			

Note: (+) Major detected minerals; (**s**) secondary minerals.

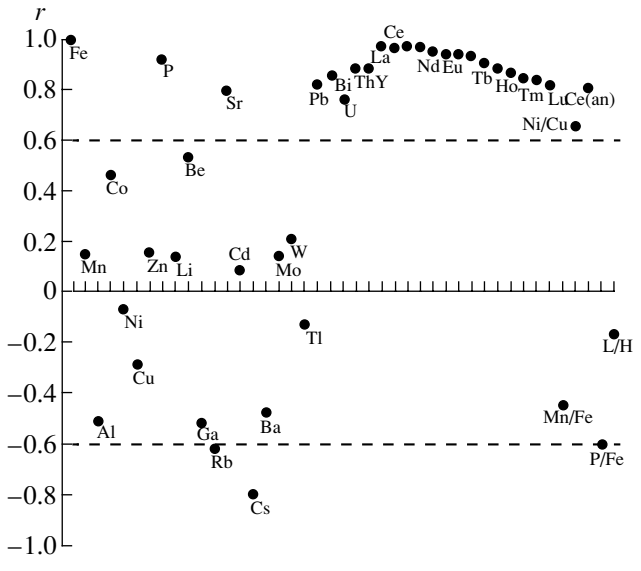

Fig. 3. Coefficients of correlation (*r*) of elements and ratios of some elements vs. Fe contents in ferromanganese nodule samples from Station 3911/76. Dashed lines show significant values of *r* (probability, $P = 0.95$; number of samples, $n = 11$).

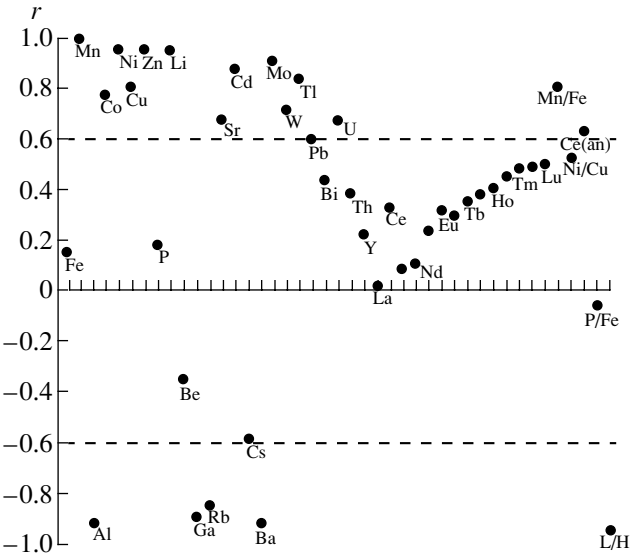

Fig. 4. Coefficients of correlation (*r*) of elements and ratios of some elements vs. Mn contents in ferromanganese nodule samples from Station 3911/76.

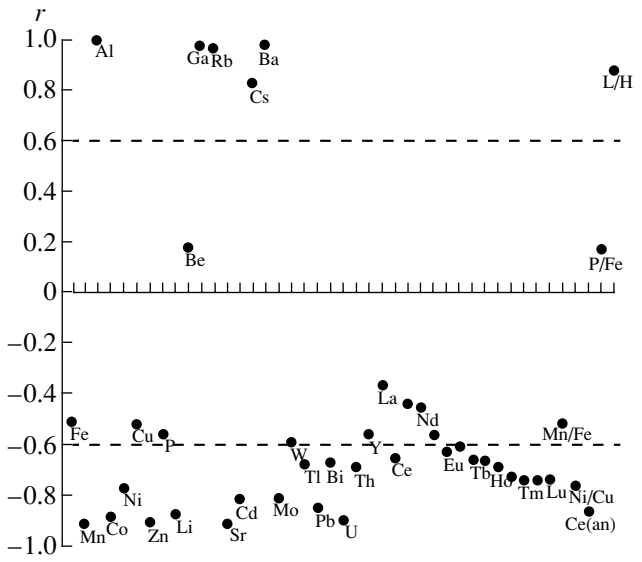

Fig. 5. Coefficients of correlation (r) of elements and ratios of some elements vs. Al contents in ferromanganese nodule samples from Station 3911/76.

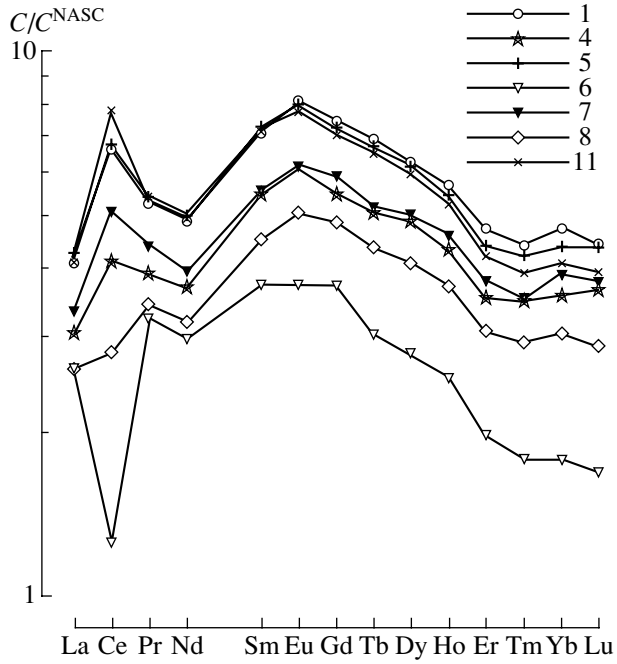

Fig. 6. NASC-normalized REE distribution in surface layer samples of a nodule from Station 3911/76. Numbers in the legend are as in Tables 1 and 2.

(Baturin and Savenko, 1989; Dymond *et al.*, 1984; Heye and Marchig, 1977; Huh and Ku, 1984; Skornyakova *et al.*, 1993).

As was mentioned above, maximal Mn/Fe values in the ferromanganese nodule from Station 3911/76 located north of the equatorial Pacific are recorded in the bottom water-facing parts of the nodule located above or beneath the water–sediment interface (Fig. 2). This is probably related to the successive input of Mn, which was reduced during the diagenesis, from the interstitial water to the bottom water and the adjacent nodule surface. The Mn enrichment of marginal parts of the lower part is caused by the input of Mn directly from the interstitial water. The presence of a specific belt (depression) along the nodule perimeter at the water–sediment interface testifies to a relatively low growth rate of the nodule near the surface layer owing to the input of labile organic matter and the dissolution of manganese oxyhydroxides in sediments. In the lower part, the Mn/Fe ratio (2.6–3.7) is quite comparable with that in the upper (bottom water-facing) part (2.8–3.8).

Zonality in the structure of surface layers of the nodule is well manifested in the distribution of Fe, Mn, and Mn/Fe. The Al distribution reflects the entrapment of lithogenic material from the sediment (Tables 1 and 2). The lower (sediment-facing) parts of the nodule are enriched in Al and specific microelements that are concentrated in the sediment. These microelements include primarily analogues of Al in the third group of the Periodic Table (e.g., Ga) and alkaline and alkaline earth (Rb, Cs, and Ba) elements. Concentration of clayey material in lower parts of the nodule is indicated by their mineral compositions (Table 2). Aluminosilicates have been detected in samples 4–8. Their concentration is very high in Sample 6.

Samples 1–3 from upper parts of the nodule contain a small amount of the authigenic nontronite with a simplified composition corresponding to $[Fe_2Si_4O_{10}(OH)_2 \cdot nH_2O]$. Its presence testifies to the following diagenetic reactions on the nodule surface:

$$2FeOOH + 4SiO_2 \cdot nH_2O \Rightarrow Fe_2Si_4O_{10}(OH)_2 \cdot nH_2O.$$

Reaction of Fe with the amorphous biogenic SiO_2 is typical of oceanic sediments, particularly in the radiolarian zone of the Peru Basin in the Pacific (Cole, 1985; Dymond and Eklund, 1978; Haese, 2000; Severmann *et al.*, 2004). Accomplishment of this reaction, probably, requires the preliminary removal of Mn as a result of its reduction by organic matter from ferromanganese oxyhydroxide intergrowths. Authigenic aluminosilcates (e.g., zeolites) can be formed on the ferromanganese oxyhydroxide surface. The formation of such aluminosilicates on the hydrogenous ferromanganese crust owing to the halmyrolysis of volcaniclastic material therein has been reported from the South Pacific Basin (Dubinin, 1998b). The Mn content in the surface layer is approximately time times lower (1.14%) than that in the lower layer of the crust, but the Fe content is similar in both cases. Decrease in the Mn content is related to reduction of Mn by the bivalent Fe of the volcaniclastic material.

The surface layer of the examined nodule is characterized by abundance of a ferruginous phase Fe-X that includes a significant amount of Si. The SEM analysis showed that the Si content is strongly variable at different points. The Fe-X phase is usually recorded as a

minor component in pelagic nodules. The structure of this phase has not been identified so far because of its minor content, fine-dispersed state, intricate association with other minerals (amorphous silica and aluminosilcates), and low degree of crystallinity. According to Chukhrov *et al.* (1987), the Fe-X phase represents a disordered intergrowth of ultrafine structural fragments of lepidocrocite and hematite. This phase is primarily observed in Fe-rich nodule samples with lower Mn/Fe values. It is quite possible that the Fe-X phase is a product of the decomposition (diagenetic alteration) of hydrogenous ferromanganese oxyhydroxides. Hence, the presence of nontronite in surface layers of the nodule suggests the reduction of Mn by the suspended organic matter and the subsequent interaction of iron oxyhydroxides with the biogenic opal.

The ore material is mainly composed of Fe-vernadite and Fe-poor vernadite. Subordinate minerals are represented by manganese minerals (asbolane-buserite and birnessite) that are typical of diagenetic nodules. The relative concentration of Mn-rich minerals (Fe-poor vernadite, birnessite, and asbolane-buserite) is observed in lateral zones of the surface layer of the nodule (samples 2–4, 7–9), where the Mn/Fe ratio is maximal (3.7–5.6). The upper and lower parts of the surface zone of the studied nodule (Mn/Fe = 3 or less) is primarily enriched in Fe-vernadite, whereas concentrations of Fe-poor vernadite and Fe-X phase are less significant.

In terms of contents of Fe, Mn, and (Co + Ni + Cu), the studied nodule samples belong to sedimentary–diagenetic formations (Skornyakova, 1986). The Co/Ni ratio varies from 0.14 to 0.34 (Table 1). Maximal Co/Ni values (0.27–0.34) are recorded at the upper surface, while minimal values (0.14–0.17) are observed in the surface layers of the nodule submerged in the sediment. Such behavior of Ni and Co is related to their fractionation in oceanic water due to oxidation of Co^{2+} into Co^{3+} after the sorption by manganese oxyhydroxides from surface waters (Moffett and Ho, 1996). In the course of reduction of Mn during the early diagenesis, Co is also reduced and usually removed from the diagenetic manganese oxyhydroxides. The contribution of diagenesis to Mn accumulation has a positive correlation with the Mn/Fe ratio and a negative correlation with the Co accumulation. Cu and Zn are present in structures of diagenetic manganese minerals. However, their concentration depends on the rate and intensity of diagenesis and is independent of the primary composition of suspended manganese oxyhydroxides (Dymond *et al.*, 1984).

In order to calculate the input of material into ferromanganese formations during diagenesis and sedimentation, it is preferential to use microelements of the iron group that are low mobile in the diagenesis. The trivalent Fe is not reduced under equilibrium conditions of the tetravalent Fe reduction by organic matter. Low-crystalline oxyhydroxides of Fe^{3+} can only be transformed into ferromanganese aggregates owing to the migration of colloidal particles. The Mn/Fe value increases in diagenetic ore aggregates, because mobility of Fe in the colloidal form is much less than that of Mn in the true dissolved from Mn^{2+} (Volkov, 1979; Punin *et al.*, 1995).

Suspended matter of iron oxyhydroxides adsorbs mainly multicharge cations (Y, REE, Th, Zr, and Hf) or oxyanions (Si, P, As, and Se), which make up low-soluble compounds (e.g., hydroxophosphates and silicates), from the oceanic water (Dubinin, 1998b; Feely *et al.*, 1991; Koschinsky and Halbach, 1995). Together with Fe, microelements that are *rigidly* bound with iron oxyhydroxides and dispersed in the sediment are transformed into accretions (micronodules and nodules) and retain the memory of primary sources.

Additional accumulation of Mn in the nodule near the water–sediment interface provokes decrease in contents of Fe, REE, Th, Y, Bi, Pb, P, and U. The REE series demonstrates certain zonality: the heavier the element, the higher the coefficient of correlation with Mn (Fig. 4) and Mn/Fe. Aluminum shows an inverse relationship: the lighter the element, the higher the coefficient of correlation (Fig. 5). The higher significance of correlation of REE and Ce with Mn and Mn/Fe is presumably related to HREE concentration in the oceanic water and Ce oxidation in manganese oxyhydroxides. The Ce anomaly shows an inverse correlation with Mn/Fe (Fig. 2). Maximal values of Ce anomaly (1.34–1.70) are recorded not only in the upper (bottom water-facing) part of the nodule, but also in the lower part (1.40–1.44). Sample 6 shows a negative Ce anomaly similar to that in the associated sediments (Table 3, Fig. 7). Taking into consideration similar contents of Fe and Al in Sample 6 and the adjoining sedimentary layer at 2–7 cm (Tables 1 and 3), one can assume that the REE spectrum in Sample 6 represents the total REE spectrum in the nodule-hosted oxyhydroxides and associated sediments.

If we assume that the content of the inert (in diagenesis) Al in Sample 6 is a simple mixing of ore oxyhydroxides and associated sediments, the Al content in Sample 6 can easily be expressed as the share of ore material (x) and associated sediment (y):

$$2.5x + 6.5y = 5.8,$$

where 2.5, 6.5, and 5.8% designate the average Al contents in the adjacent samples 5 and 7, the associated sediment at interval 2–7 cm (Table 3), and Sample 6, respectively. Since $x + y = 1$, we obtain $x = 0.17$. It is worth noting that estimation of the sedimentary material based on the Al content will be underestimated, because not the whole Al in oxyhydroxides is represented by the lithogenic component. Relationship between the sedimentary and ore materials may be more precisely calculated based on the Mn content, because its share is negligible in the lithogenic material. After calculating the average for samples 5 and 7, we obtain the Mn content in the ore material (21.5%). Taking into consideration the Mn concentration in Sample 6

Table 3. Contents of elements in manganese micronodules and associated sediments at Station 3911/76 (Dubinin and Sval'nov, 2003)

Elements	Size of ferromanganese nodules, μm				Associated sediment, interval (cm)	
	50–100	100–250	250–500	>500	0–2	2–7
La	45.4	38.4	35.1	41.7	56.5	51.3
Ce	345	183	144	152	106	87.3
Pr	16.2	13.6	12.7	15.7	17.3	15.3
Nd	67.1	57.3	54.7	66.3	68.3	60.8
Sm	16.7	15.0	15.4	18.1	17.1	15.0
Eu	3.75	3.68	3.53	4.21	4.20	3.49
Gd	14.4	13.7	13.5	16.9	17.8	15.4
Tb	2.16	2.09	1.97	2.47	2.74	2.26
Dy	11.6	10.9	10.5	13.1	15.6	13.9
Ho	1.94	1.90	1.86	2.36	3.03	2.74
Er	4.98	4.97	4.68	5.69	8.07	7.29
Tm	0.77	0.73	0.69	0.84	1.13	1.05
Yb	4.83	4.61	4.21	5.60	7.29	6.85
Lu	0.69	0.65	0.63	0.82	1.09	1.02
Mo	401	574	587	561	63	5.0
W	86	54	64	56	12.5	5.3
Th	16.3	9.10	7.72	9.09	11.9	13.4
Al	1.16	2.01	1.82	1.65	5.50	6.49
Ti	1.49	0.24	0.24	0.43	0.34	0.39
Fe	6.67	2.61	2.13	2.85	3.91	4.25
Mn	23.2	21.4	24.3	27.6	3.17	0.29
Ni	1.13	1.44	1.41	1.42	n.d.	n.d.
Co	0.10	0.16	0.11	0.12	n.d.	n.d.
Cu	1.23	1.59	1.69	1.63	n.d.	n.d.
P	0.169	0.101	0.087	0.068	0.135	0.123
Mn/Fe	3.47	8.20	11.4	9.68	0.81	0.07
P/Fe	0.025	0.039	0.041	0.024	0.034	0.029
Ce(an)	2.73	1.72	1.46	1.27	0.74	0.68

Note: Contents of REE, Mo, W, and Th are given in ppm; other elements, in %. (n.d.) Not determined.

(6.4%) and associated sediments at interval 2–7 cm (0.3%), we obtain

$$21.5x + 0.3y = 6.4.$$

Solution of this equation yields $x = 0.29$. Calculation of REE contents in Sample 6 with the consideration of the contribution of ore and lithogenic components is shown in Fig. 7. Data on the Mn distribution show a satisfactory coincidence of calculated and measured concentrations of REE (except Ce). On the whole, the mixing model of the ore material and associated sediment does not reproduce the REE spectrum in Sample 6 (Fig. 7). Sample 6 is enriched in LREE relative to the associated sediment at interval 2–7 cm. The simple subtraction of REE contents in the associated sediment from the average value for samples 5 and 7 yields a value that is surprisingly similar with the value for Sample 6 (in terms of REE contents and spectrum, except for Ce). Presumably, the REE spectrum in this sample taken from the lower surface of the nodule represents a mixing of REE spectrums in diagenetic ferromanganese oxyhydroxides and associated sediments. If this assumption is correct, the diagenetic ferromanganese oxyhydroxides should primarily be characterized by deficit of Ce and HREE.

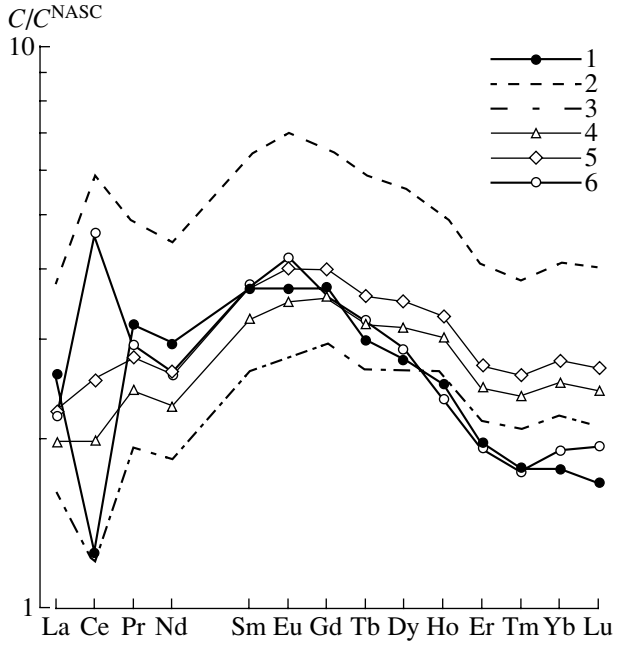

Fig. 7. NASC-normalized REE distribution. (1) Sample 6; (2) average for the oxyhydroxide material in samples 5 and 7; (3) associated sediment at interval 2–7 cm; (4, 5) REE spectrum in the mixing model: (4) at ore material content equal to 0.17 (based on Al), (5) at ore material content equal to 0.29 (based on Mn); (6) REE spectrum based on subtraction of REE in the associated sediment from the nodule ore material (samples 5 and 7).

If we omit the anomalous Sample 6 from further consideration, Ce, Th, and Nd contents apparently show a significant negative correlation with the Mn/Fe ratio that characterizes the diagenetic accumulation of Mn (Fig. 8). This fact testifies to low mobility of these elements in the course of diagenesis due to the low mobility of colloidal forms of iron oxyhydroxides that served as the sorbent.

When Mn is reduced and removed from the surface of hydrogenous oxyhydroxide particles, the newly formed surface of iron oxyhydroxides will be undersaturated, relative to equilibrium contents of phosphates and silicates in the bottom and interstitial waters. This leads to the sequential sorption and formation of not only iron oxyhydroxides, i.e., growth in the P/Fe ratio (Dubinin, 2001), but also iron silicates (nontronite). The P/Fe versus Mn/Fe relationship (Fig. 9) is related precisely to this process rather than the accumulation of phosphorus on Mn(IV) oxyhydroxides (Balistrieri and Chao, 1990). Authigenic silicates do not accumulate REEs (Stoffers *et al.*, 1985; Volkov and Dubinin, 1987), while hydroxophosphates can foster the sorptional activity of iron oxyhydroxide particles relative to the REEs. The consequent additional sorption of REEs on phosphate particles from the bottom and interstitial waters changes the initial REE spectrum of hydrogenous oxyhydroxide particles. Rare earth elements in nodules of the radiolarian zone are mainly related to iron oxyhydroxides and

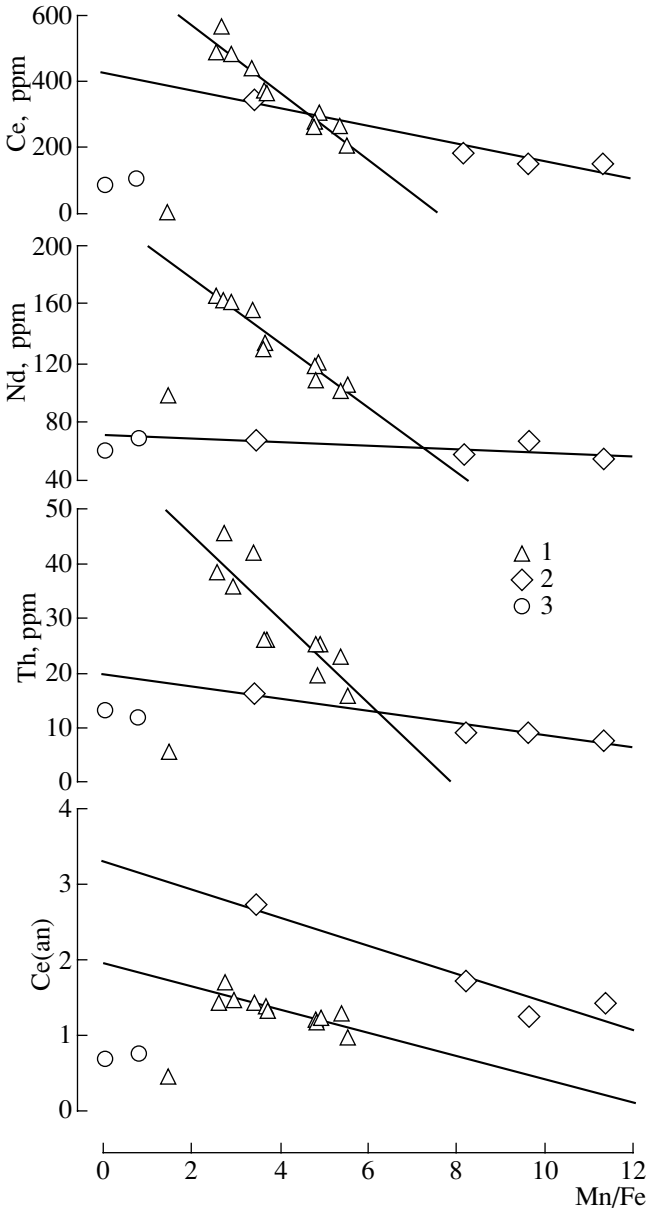

Fig. 8. Variations in Ce, Th, Nd, and Ce(an) vs. Mn/Fe in (1) ferromanganese nodule, (2) micronodules of different fractions, and (3) associated sediments at Station 3911/76.

hydroxophosphates (Dubinin *et al.*, 1997; Elderfield *et al.*, 1981). Relationship between these phases in the nodule governs Ce anomaly in the REE spectrum. Sedimentary nodules are characterized by Ce(an) > 1, whereas diagenetic and diagenetic–sedimentary varieties are marked by Ce(an) < 1. Since the Ce anomaly in iron oxyhydroxides and hydroxophosphates are characterized by positive and negative signs, respectively, we supposed that the hydroxophosphate phase prevails in the composition of diagenetic nodules (Dubinin and Sval'nov, 2003; Dubinin *et al.*, 1997). Figure 8 shows that the Mn/Fe has a negative correlation with the Ce(an) value within a single nodule from the radiolarian zone. This may be a response not to the

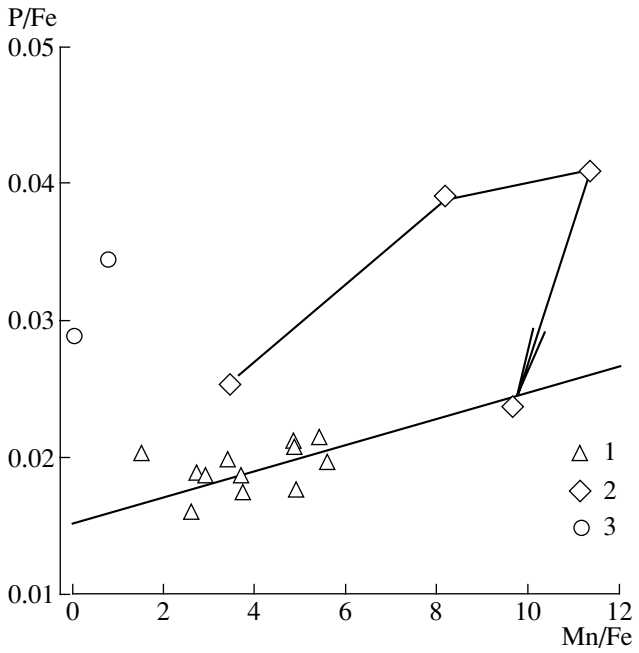

Fig. 9. P/Fe vs. Mn/Fe relationship in (1) nodule samples, (2) micronodules, and (3) associated sediments. Arrows show the direction of increase in the size of micronodule fractions.

diagenetic accumulation of Mn, but to variation in the composition of iron oxyhydroxides, their partial transition to hydroxophosphates and silicates, and sorption of REEs from the bottom and interstitial waters that are characterized by Ce deficit (Dubinin, 2004; Haley *et al.*, 2004).

Relationship between Compositions of Ferromanganese Nodules and Manganese Micronodules

Manganese micronodules are products of diagenetic reactions in the sediment. Variations in the composition and size of micronodules depend only on the degree of diagenetic transformation of ferromanganese oxyhydroxides (Dubinin and Sval'nov, 1995, 1996, 2000a, 2000b, 2003). In zones with high bioproductivity of oceanic water, the Ce anomaly in the REE spectrum has a negative correlation with the size of micronodules due to a higher role of the reactive part of sediment during the formation of micronodules in the course of early diagenesis. This is accompanied by increase in Mn/Fe and P/Fe values (Fig. 9). The timing of the surface layer of the nodule (<2 mm) can be quite comparable with the formation and growth period of micronodules (maximal size up to 2 mm). However, the micronodules and lower layers of the nodule can grow at different times.

Manganese micronodules from Station 3911/76 (interval 0–7 cm) and associated sediments from intervals 0–2 and 2–7 cm have been scrutinized in our previous work (Dubinin and Sval'nov, 2003). The above work also presented data on the bulk composition of nodule that was similar to the nodule considered in the present communication in terms of morphology, size, and composition. Sediments at interval 0–2 cm are enriched in Mn (3.17%) relative to the underlying layer (0.29%) owing to diagenesis. The sediment interval used for micronodule selection exceeded the depth of nodule subsidence into the sediment, because we were forced to include the interval of 0–7 cm in order to obtain a sufficient micronodule material for the analysis.

Micronodule fraction >500 μm slightly differed from the general trend of compositional variation depending on grain size distribution and was similar to the nodule (Fig. 9). Therefore, we assumed that the fraction included a higher content of hydrogenous material owing to the direct precipitation of suspended matter or the introduction of nodule material due to its crushing (Dubinin and Sval'nov, 2003). Figure 9 shows the P/Fe–Mn/Fe relationship in associated sediments, micronodules, and macronodules. One can see that the P/Fe ratio in the nodule and micronodules depends on the input of diagenetic Mn. It is also evident that the micronodules are more affected by the influence of diagenesis than the nodules, in which the P/Fe value directly depends on the Mn/Fe ratio. This trend is also typical of three micronodule fractions, except the coarsest fraction. However, relative to the nodules, the micronodules are characterized by higher values and wider variation ranges of Mn/Fe and P/Fe ratios.

The micronodule material is significantly altered by diagenesis. This is also indicated by the lower values of Ni/Cu (0.87–0.92) and Co/Ni (0.08–0.09) in the micronodules, relative to nodules (1.23–1.97 and 0.14–0.34, respectively). The Ni/Cu and Co/Ni ratios were not considered for Sample 6.

Increase in the P/Fe value with intensification of the influence of diagenesis testifies to the compositional variation in iron oxyhydroxides. As was mentioned above, the removal of Mn from ferromanganese oxyhydroxide intergrowths leads to qualitative changes in authigenic iron minerals—increase in the share of iron hydroxophosphates and, probably, silicates (nontronites). The compositional variation in authigenic iron minerals provokes the redistribution of microelements between the newly formed phases of iron phosphates and silicates. High-field strength cations of Th and Ce (charge 4^+) belong to the group of the least mobile elements associated with Fe in postsedimentary environments. In terms of the Th–Ce relationship (Fig. 10), the ferromanganese nodules does not differ from the micronodules, although concentrations of these elements in the micronodules are lower because of decrease in the Fe content relative to the nodules. According to (Moore, 1984), ^{230}Th and ^{232}Th show a linear relationship in nodules, micronodules, and associated sediments of the equatorial Pacific (MANOP Site S). Isotope ^{230}Th is a product of ^{234}U decay.

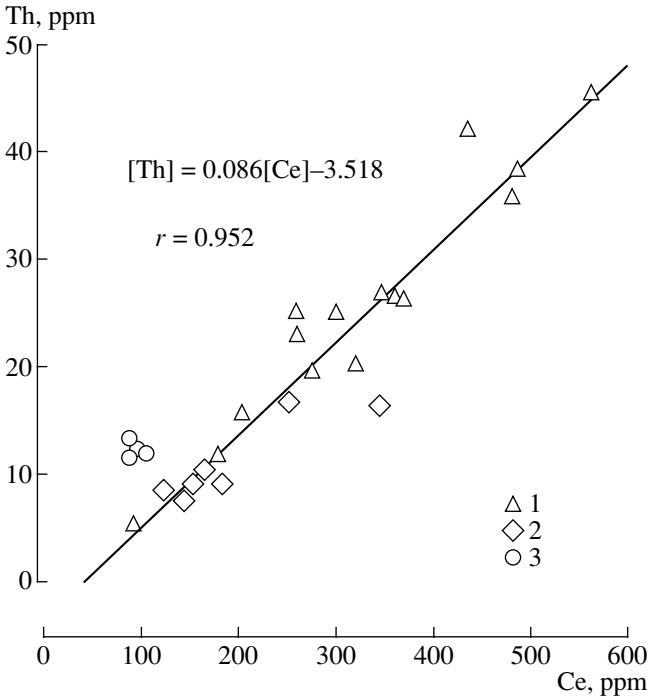

Fig. 10. Th vs. Ce relationship in (1) ferromanganese nodules, (2) manganese micronodules, and (3) associated sediments at Stations 3911/76 and 3915. Data on Station 3915 are adopted from (Dubinin and Sval'nov, 2003).

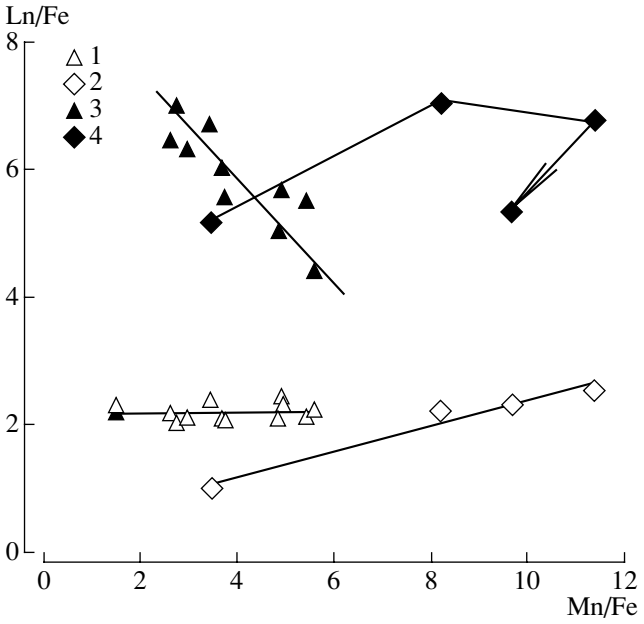

Fig. 11. Variations in (1, 2) Nd and (3, 4) Ce contents ($n \times 10^{-3}$) vs. Fe content in samples of (1, 3) ferromanganese nodule and (2, 4) manganese micronodule.

Increase of the $^{230}Th/^{232}Th$ ratio can be related to the accumulation of excess ^{230}Th on ferromanganese oxyhydroxide particulates due to the radioactive decay of U in oceanic water. Difference in the behavior of ^{230}Th and ^{232}Th in deep zones of the Pacific Ocean was reported in (Roy-Barman *et al.*, 1996).

In the northern equatorial Pacific, relative to lower parts of nodules, the upper parts show higher $^{230}Th/^{232}Th$ values that are similar to those in deep waters (Moore, 1984). Relative to the micronodules, the nodules are characterized by greater slope of the regression line, which reflects the $^{230}Th/^{232}Th$ variation in nodules, and higher content of ^{230}Th. In contrast, the associated sediments show lesser slope of the regression line, relative to the micronodules. This is presumably related to the share of hydrogenous iron oxyhydroxides in the studied sediments. At MANOP Site S, nodules are characterized by the highest content of hydrogenous iron oxyhydroxides. In all 11 samples of the ferromanganese nodule, the average U/Th ratio is 0.17 ± 0.04, which is consistent with the data on nodules from MANOP Site S (Dymond *et al.*, 1984).

Since nodules and micronodules are differently altered in the course of diagenesis, based on Mn/Fe (Fig. 9) and $^{230}Th/^{232}Th$ values, one can affirm that the Th/Ce ratio is constant for sediments from stations 3911/76 and 3915 (Fig. 10); i.e., this ratio is not subjected to changes in the course of diagenetic reactions and was already stabilized at the stage of suspension in the oceanic water. The associated sediments are enriched in Th relative to Ce.

Variations in contents of Th, Ce, and Nd, relative to Mn/Fe, in nodules, micronodules, and associated sediments are shown in Fig. 8. One can see a negative correlation of Ce and Th with Mn/Fe. However, the slope of regression line is different in the nodules and micronodules. Relative to micronodules, nodules are marked by a faster decrease in contents of Th and Ce with increase in Mn/Fe. The Nd content also shows a negative correlation with Mn/Fe. In the micronodules, the Nd content is virtually constant, although the Fe content decreases (Table 3).

Compositional variations in iron oxyhydroxides in the course of early diagenesis can be characterized by variations in relationships between microelements and Fe. The composition of upper parts, which best reflect the composition of sedimentary oxyhydroxides, indicate that the Ce/Fe ratio has a negative correlation with Mn/Fe (Fig. 11). Increase in the size of micronodules is accompanied by the successive increase and decrease in the Ce/Fe value. The Ce/Fe ratio is similar in the micronodules and nodules. At the same time, the Nd/Fe ratio does not depend on Mn/Fe in the nodule and slightly increases with the diagenetic accumulation of Mn.

The anomalous behavior of Ce (relative to trivalent REE) is expressed in the Ce anomaly value (Fig. 8). This value shows negative correlation with Mn/Fe and micronodule dimension. Although the Ce(an)–Mn/Fe relationship in nodules and micronodules is similar, the difference between Ce(an) values with increase in Mn/Fe is nearly constant (1.5). Relative to nodules,

micronodules have a higher Ce anomaly not only in the radiolarian belt, but also in the Peru and Guatemala basins. These distinctions are typical of bioproductive zones in the ocean (Dubinin and Sval'nov, 1995, 1996, 2000a, 2000b, 2003).

Calculation formulas presented above show that the Ce anomaly depends on not only Ce accumulation, but also La and Nd contents. Hence, the negative correlation between Ce(an) and Mn/Fe can be related to both increase in the Ce content and increase in La and Nd contents. Figure 8 suggests that both Ce and Nd contents in the nodule have negative correlation with Mn/Fe. Decrease in the Nd content is less prominent, relative to Ce. This is shown by decrease in the Ce(an) value. The higher decrease in Ce content may be caused by the reduction of Mn during diagenesis, because a certain part of Ce is located in manganese oxyhydroxides owing to the oxidation of Mn and Ce in upper layers of the oceanic water. Our data show that approximately 25% of the total Ce content is linked with manganese oxyhydroxides in the hydrogenous crust of the South Pacific Basin (Dubinin, 1998b). Decrease of the Nd content in the nodule is probably related to its dilution by the additional input of diagenetic Mn. This conclusion is confirmed by the distribution of Nd/Fe and Ce/Fe relative to Mn/Fe (Fig. 11). The Ce/Fe value decreases, while the Nd/Fe remains virtually constant. Cerium reduced in the course of diagenesis is again oxidized after the sorption on iron oxyhydroxides and its behavior becomes similar to that of Th.

The behavior of Ce and Nd is different in the micronodules. In iron oxyhydroxides, the Ce/Fe value is similar to that in the nodule, whereas the Nd/Fe value grows with increase in Mn/Fe. It is known that contents of trivalent REEs in micronodules from the oceanic bioproductive zone are always lower than in the coexisting nodules, while the Ce content is similar to that in nodules (Dubinin and Sval'nov, 1995, 1996, 2000a, 2000b, 2003). Therefore, relative to nodules, micronodules from the bioproductive zones are always characterized by higher Ce(an) values (Fig. 8).

The Ce–Th relationship is rather universal for the oceanic ferromanganese oxyhydroxides and can be defined by the very low mobility of Ce and Th of oxidation state 4^+, the deficit of Ce relative to trivalent REEs in deep waters, and the Ce–Th relation in the oceanic surface water. Under conditions of close intergrowth of manganese and iron oxyhydroxides, the trivalent REEs (Nd, in particular) are adsorbed on oxyhydroxide surfaces. If Mn is reduced, the iron oxyhydroxide surface is transformed in the course of diagenesis owing to the specific sorption of phosphate ion and subordinate SiO_2. The oceanic trivalent REEs are characterized by their accumulation on phosphate surfaces (Dubinin, 2004). This is indicated by high contents of trivalent REEs in the bone detritus and iron hydroxophosphates, correlation between P and REEs in the oceanic sediments, and abundance of REEs associated with the authigenic phosphate in sediments of the radiolarian zone (Dubinin *et al.*, 1997; Elderfield *et al.*, 1981).

Relative to iron, phosphorus has a lower "compressibility" if we define this property as the ratio of P contents in nodules and in the reactive portion of the associated sediments (Volkov, 1979). The authigenic phosphate (iron hydroxophosphate) is more readily accumulated in sediments than in nodules. Therefore, the related trivalent REEs mainly remain in the sediments, and sometimes the content of trivalent REEs in the sediments turns out to be higher than that in the diagenetic nodules (Dubinin *et al.*, 1997). Hence, higher Ce(an) values in micronodules (relative to nodules) are related to the redistribution of REEs, which are adsorbed on the hydrogenous iron oxyhydroxides, between iron oxyhydroxides and hydroxophosphates in the course of diagenesis. Moreover, the accumulation of P on iron oxyhydroxides during the early diagenesis of sediments leads to increase of the P/Fe value in micronodules with increase in their size and input of diagenetic matter (Fig. 9).

Differences in the chemical composition of nodules and micronodules described above are probably typical of bioproductive zones of the ocean. The degree of their manifestation depends on the amount of labile organic matter that reaches the bottom, rates of sedimentation and ore formation, and the presence of biogenic silica. The rates of sedimentation and ore formation significantly govern the accumulation of phosphates on iron oxyhydroxides and, correspondingly, the role of iron oxyhydroxides in the REE redistribution.

CONCLUSIONS

Processes of ore formation in the radiolarian belt of sedimentation in the northern Pacific have been considered based on the study of surface layer (<2 mm) samples of a sedimentary-diagenetic ferromanganese nodule and four size fractions of manganese micronodules extracted from the associated surface sediment (0–7 cm). The ferromanganese nodule is characterized by compositional inhomogeneity in space. The Mn/Fe ratio is maximal in samples taken from lateral parts located immediately above and beneath the sediment surface, suggesting that the nodule growth rate was maximal along the bottom water–sediment interface due to the additional input of Mn from the surface sediment layer and the introduction of the previously reduced Mn from the bottom water. Differences in the microelement signature of the nodule is related to the preferential accumulation of microelements on iron oxyhydroxides (P, Sr, Pb, U, Bi, Th, Y, and REE), manganese oxyhydroxides (Co, Ni, Cu, Zn, Cd, Mo, Tl, and W), and the lithogenic component entrapped during the nodule growth (Ga, Rb, Ba, and Cs). The REE spectrum is characterized by high contents of MREEs and variable Ce(an) values relative to the NASC. The Ce(an) value is maximal in upper and lower parts of the nodule where the Mn/Fe ratio is minimal.

The compositional comparison of micronodules and surface samples of the nodule demonstrated that the micronodule material was more intensely reworked during the early diagenesis. The micronodules are characterized by higher Mn/Fe and P/Fe ratios but lower Ni/Cu and Co/Ni ratios. The micronodules and nodules do not differ in terms of contents of elements that are least mobile during the diagenesis of elements (Ce and Th). The Ce(an) value in the micronodules is systematically higher than that in the nodule, although this value decreases with increase in Mn/Fe in both cases. Differences in the chemical composition of micronodules and nodules are related to not only the additional input of Mn in the course of diagenesis in the sediment and nodule surface, but also to the transformation of iron oxyhydroxides after the removal of Mn from the close association with ferromanganese oxyhydroxides developed at the suspension stage in the course of sedimentation. The additional sorption of phosphate ion by iron oxyhydroxides and the reaction with biogenic opal leads to decrease in its compressibility and the redistribution of microelements between the oxyhydroxide, phosphate, and silicate phases of authigenic iron minerals. A part of trivalent REEs is transferred into iron oxyhydroxides in the sediments owing to increase of Ce anomaly in the micronodules relative to the nodules.

ACKNOWLEDGMENTS

This work was supported by the Russian Foundation for Basic Research, project no. 04-05-65104.

REFERENCES

Anufriev, G.S., Boltenkov, B.S., Volkov, I.I., and Kapitonov, I.N., Determination of Growth Rate of Oceanic Ferromanganese Nodules Based on Helium and Neon Stable Isotopes, *Litol. Polezn. Iskop.*, 1996, vol. 31, no. 1, pp. 3–11 [*Lithol. Miner. Resour.* (Engl. Transl.), 1996, vol. 31, no. 1, pp. 1–8].

Balistrieri, L.S. and Chao, T.T., Adsorption of Selenium by Amorphous Iron Oxyhydroxide and Manganese Dioxide, *Geochim. Cosmochim. Acta*, 1990, vol. 54, no. 3, pp. 739–751.

Baturin, G.N., *Geokhimiya zhelezomargantsevykh konkretsii okeana* (Geochemistry of Oceanic Ferromanganese Nodules), Moscow: Nauka, 1986.

Baturin, G.N. and Savenko, V.S., Growth Rates of Deep-Water Ferromanganese Nodules, *Okeanologiya*, 1989, vol. 29, no. 3, pp. 442–452.

Chukhrov, F.V., Drits, V.A., Gorshkov, A.I., *et al.*, Structural Models of Vernadite, *Izv. Akad. Nauk SSSR, Ser. Geol.*, 1987, no. 12, pp. 3–16.

Cole, T.G., Composition, Oxygen Isotope Geochemistry, and Origin of Smectite in the Metalliferous Sediments of the Bauer Deep, Southeast Pacific, *Geochim. Cosmochim. Acta*, 1985, vol. 49, no. 1, pp. 221–235.

Dubinin, A.V., The Inductively Coupled Plasma Mass Spectrometry: Determination of Rare Earth Elements in Standard Samples of Oceanic Sediments, *Geokhimiya*, 1993, vol. 31, no. 11, pp. 1605–1619.

Dubinin, A.V., Rare Earth Elements during the Early Diagenesis of Sediments in the Pacific Ocean, *Litol. Polezn. Iskop.*, 1998a, vol. 33, no. 4, pp. 762–772 [*Lithol. Miner. Resour.* (Engl. Transl.), 1998a, vol. 33, no. 4, pp. 304–312].

Dubinin, A.V., Ferromanganese Crust on Pelagic Sediments: Geochemistry and Formation Conditions, *Geokhimiya*, 1998b, vol. 36, no. 11, pp. 1152–1163 [*Geochem. Int.* (Engl. Transl.), 1998b, vol. 36, no. 11, pp. 1041–1051].

Dubinin, A.V., Geochemistry of Fe–Ca Hydroxophosphates in Pelagic Sediments: Genesis and Compositional Evolution in the Diagenesis, *Geokhimiya*, 2001, vol. 39, no. 6, pp. 645–657 [*Geochem. Int.* (Engl. Transl.), 2001, vol. 39, no. 6, pp. 585–596].

Dubinin, A.V., Geochemistry of Rare Earth Elements in the Ocean, *Litol. Polezn. Iskop.*, 2004, vol. 39, no. 4, pp. 339–358 [*Lithol. Miner. Resour.* (Engl. Transl.), 2004, vol. 39, no. 4, pp. 289–307].

Dubinin, A.V. and Strekopytov, S.V., Geochemistry of Rare Earth Elements during the Formation of Ferromanganese Nodules in the Peru Basin of the Pacific, *Litol. Polezn. Iskop.*, 1994, vol. 29, no. 4, pp. 17–32.

Dubinin, A.V. and Strekopytov, S.V., Investigation of the Behavior of Rare Earth Elements during the Leaching of Oceanic Sediments, *Geokhimiya*, 2001, vol. 39, no. 7, pp. 762–772 [*Geochem. Int.* (Engl. Transl.), 2001, vol. 39, no. 7, pp. 692–701].

Dubinin, A.V. and Sval'nov, V.N., Micronodules in the Guatemala Basin: Geochemistry of Rare Earth Elements, *Litol. Polezn. Iskop.*, 1995, vol. 30, no. 5, pp. 473–479.

Dubinin, A.V. and Sval'nov, V.N., Differential Mobility of Iron Oxyhydroxides during the Formation of Micro- and Macronodules, with the Guatemala Basin in the Pacific as an Example, *Dokl. Akad. Nauk*, 1996, vol. 348, no. 1, pp. 100–103 [*Dokl.* (Engl. Transl.), 1996, vol. 348, no. 4, pp. 615–618].

Dubinin, A.V. and Sval'nov, V.N., Geochemistry of Rare Earth Elements in Micro- and Macronodules from the Pacific Bioproductive Zone, *Litol. Polezn. Iskop.*, 2000a, vol. 35, no. 1, pp. 25–39 [*Lithol. Miner. Resour.* (Engl. Transl.), 2000a, vol. 35, no. 1, pp. 19–31].

Dubinin, A.V. and Sval'nov, V.N., Geochemistry of Rare Earth Elements in Ferromanganese Micro- and Macronodules from the Pacific Nonproductive Zone, *Litol. Polezn. Iskop.*, 2000b, vol. 35, no. 6, pp. 586–604 [*Lithol. Miner. Resour.* (Engl. Transl.), 2000b, vol. 35, no. 6, pp. 520–537].

Dubinin, A.V. and Sval'nov, V.N., Geochemistry of the Manganese Ore Process in the Ocean: Evidence from Rare Earth Elements, *Litol. Polezn. Iskop.*, 2003, vol. 38, no. 2, pp. 115–125 [*Lithol. Miner. Resour.* (Engl. Transl.), 2003, vol. 38, no. 2, pp. 91–100].

Dubinin, A.V., Skornyakova, N.S., Strekopytov, S.V., and Volkov, I.I., Geochemistry of Rare Earth Elements in Nodules and Host Sediments in the Northern Equatorial Pacific, *Litol. Polezn. Iskop.*, 1997, vol. 32, no. 2, pp. 199–211 [*Lithol. Miner. Resour.* (Engl. Transl.), 1997, vol. 32, no. 2, pp. 172–183].

Dymond, J. and Eklund, W., A Microprobe Study of Metalliferous Sediment Components, *Earth Planet. Sci. Lett.*, 1978, vol. 40, no. 2, pp. 243–251.

Dymond, J., Lyle, M., Finney, B., *et al.*, Ferromanganese Nodules from MANOP Sites H, S and R—Control of Mineralogical and Chemical Composition by Multiple Accretion-

ary Processes, *Geochim. Cosmochim. Acta*, 1984, vol. 48, no. 5, pp. 931–949.

Elderfield, H., Hawkesworth, C.J., Greaves, M.J., and Calvert, S.E., Rare Earth Element Zonation in Pacific Ferromanganese Nodules, *Geochim. Cosmochim. Acta*, 1981, vol. 45, no. 7, pp. 1231–1234.

Feely, R.A., Trefry, J.H., Massoth, G.J., and Metz, S., A Comparison of the Scavenging of Phosphorus and Arsenic from Seawater by Hydrothermal Iron Oxyhydroxides in the Atlantic and Pacific Oceans, *Deep-Sea Res.*, 1991, vol. 38, no. 6, pp. 617–623.

Gromet, L.P., Dymek, R.F., Haskin, L.A., and Korotev, R.L., The "North American Shale Composite": Its Compilation, Major and Trace Element Characteristics, *Geochim. Cosmochim. Acta*, 1984, vol. 48, no. 12, pp. 2469–2482.

Haese, R.R, The Reactivity of Iron, in *Marine Geochemistry*, Schulz, H.D. and Zabel, M., Eds., Berlin: Springer, 2000, pp. 233–261.

Haley, B.A., Klinkhammer, G.P., and McManus, J., Rare Earth Elements in Pore Waters of Marine Sediments, *Geochim. Cosmochim. Acta*, 2004, vol. 68, no. 6, pp. 1265–1279.

Heye, D. and Marchig, V., Relationship between the Growth Rate of Manganese Nodules from the Central Pacific and Their Chemical Constitution, *Mar. Geology*, 1977, vol. 23, pp. M19–M25.

Huh, C. and Ku, T., Radiochemical Observations on Manganese Nodules from Three Sedimentary Environments in the North Pacific, *Geochim. Cosmochim. Acta*, 1984, vol. 48, no. 5, pp. 951–963.

Koschinsky, A. and Halbach, P., Sequential Leaching of Marine Ferromanganese Precipitates: Genetic Implications, *Geochim. Cosmochim. Acta*, 1995, vol. 59, no. 24, pp. 5113–5127.

Lyle, M., Estimating Growth Rates of Ferromanganese Nodules from Chemical Compositions: Implications for Nodule Formation Process, *Geochim. Cosmochim. Acta*, 1982, vol. 46, no. 11, pp. 2301–2306.

Moffett, J.W., Microbially Mediated Cerium Oxidation in Sea Water, *Nature*, 1990, vol. 345, no. 6274, pp. 421–423.

Moffett, J.W. and Ho, J., Oxidation of Cobalt and Manganese in Sea Water Via a Common Microbially Catalyzed Pathway, *Geochim. Cosmochim. Acta*, 1996, vol. 60, no. 18, pp. 3415–3424.

Moore, W.S., Thorium and Radium Isotopic Relationships in Manganese Nodules and Sediments at MANOP Site S, *Geochim. Cosmochim. Acta*, 1984, vol. 48, no. 5, pp. 987–992.

Punin, Yu.O., Smetannikova, O.G., Demidova, G.E., and Smol'skaya, L.S., Dynamics of the Formation of Oceanic Ferromanganese Nodules, *Litol. Polezn. Iskop.*, 1995, vol. 30, no. 1, pp. 40–50.

Roy-Barman, M., Chen, J.H., and Wasserburg, G.J., ^{230}Th-^{232}Th Systematic in the Central Pacific Ocean: The Sources and the Fates of Thorium, *Earth Planet. Sci. Lett.*, 1996, vol. 139, pp. 351–363.

Severmann, S., Mills, R.A., Palmer, M.R., and Fallick, A.E., The Origin of Clay Minerals in Active and Relict Hydrothermal Deposits, *Geochim. Cosmochim. Acta*, 2004, vol. 68, no. 1, pp. 73–88.

Sholkovitz, E.R., Landing, W.M., and Lewis, B.L., Ocean Particle Chemistry: The Fractionation of Rare Earth Elements between Suspended Particles and Seawater, *Geochim. Cosmochim. Acta*, 1994, vol. 58, no. 6, pp. 1567–1579.

Skornyakova, N.S., Local Variations of Ferromanganese Nodule Fields, in *Zhelezomargantsevye konkretsii tsentral'noi chasti Tikhogo okeana* (Ferromanganese Nodules in the Central Pacific), Moscow: Nauka, 1986, pp. 109–184.

Skornyakova, N.S., Sval'nov, V.N., and Mukhim, V.V., Buried Nodules in the Eastern Equatorial Pacific Zone, *Litol. Polezn. Iskop.*, 1993, vol. 28, no. 5, pp. 34–51.

Stoffers, P., Lallier-Verges, E., Pluger, W., *et al.*, A "Fossil" Hydrothermal Deposit in the South Pacific, *Mar. Geology*, 1985, vol. 62, pp. 133–151.

Strekopytov, S.V. and Dubinin, A.V., Determination of Zr, Hf, Mo, W, and Th in Standard Samples of Oceanic Sediments by the ICP-MS Method, *Zh. Analit. Khimii*, 1997, vol. 52, no. 12, pp. 1296–1298.

Sval'nov, V.N., *Dinamika pelagicheskogo diageneza* (Dynamics of the Pelagic Diagenesis), Moscow: Nauka, 1991.

Uspenskaya, T.Yu. and Skornyakova, N.S., *Tekstury i struktury okeanskikh zhelezo-margantsevykh konkretsii i korok* (Structures and Textures of Oceanic Ferromanganese Nodules and Crusts), Moscow: Nauka, 1991.

Volkov, I.I., Ferromanganese Nodules, in *Okeanologiya. Khimiya okeana. Geokhimiya donnykh osadkov* (Oceanology: Oceanic Chemistry. Geochemistry of Bottom Sediments), Moscow: Nauka, 1979, vol. 2, pp. 414–467.

Volkov, I.I. and Dubinin, A.V., Rare Earth Elements in Hydrothermal Ferromanganese Deposits in Oceans, *Litol. Polezn. Iskop.*, 1987, vol. 22, no. 6, pp. 40–56.